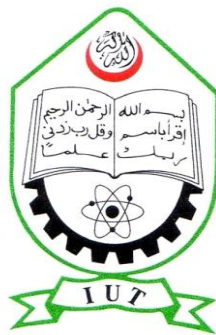


A systematic analysis on **Quickreturn Vibratory Conveyor**

by

Intesharul Haque (131433)
MD. Asif Khan Pranto (131420)
Tariqul Islam (131439)

**BACHELOR OF SCIENCE IN ELECTRICAL AND ELECTRONIC
ENGINEERING**



Department of Electrical and Electronic Engineering
Islamic University of Technology (IUT)
Gazipur, Bangladesh

Table of Contents

<u>List of Tables</u>	vi
<u>List of Figures</u>	vii
<u>List of Acronyms</u>	ix
<u>Acknowledgements</u>	xi
<u>Abstract</u>	xii
<u>1 Introduction</u>	1
<u>1.1 Basic Functionalities of</u>	1
<u>1.2 Different Aspects</u>	2
<u>1.3 Background and Motivation</u>	2
<u>2 Overview of</u>	5
<u>2.1 Introduction</u>	5
<u>2.2 Network Architecture</u>	9

Abstract

A conveyor system is a common piece of mechanical handling equipment that moves materials from one location to another. Conveyors are especially useful in applications involving the transportation of heavy or bulky materials.

A Theoretical and Experimental Study was made of the conveying speed with which the granular particles are transported by vibratory Conveyors. Layer of granular particle can be considered as a point mass. The theory will tell us about rest, slide and flight phase of the granular material.

Vibratory conveyors are highly used for discharging, conveying, feeding, dosing and distributing bulk materials in many branches of industry. The goal of our project is a systematic investigation of the dependence of the transport behavior on the principle of Quick return Linear oscillation Form. The transport velocity on the normalized acceleration is observed. Two maxima are separated by a regime, where the granular flow is much slower and, in a certain driving range, even reverses its direction.

The operation principle enables simpler manipulation tasks to be realized using an open loop setup. In this case it is not necessary to have continuous feedback of the position information of the objects on the surface, making the system quite simple. With this system, the objects can be moved along discrete, two dimensional paths and they can be moved to discrete, two dimensional locations. For many common object shapes it is also possible to influence the rotational orientation of the objects about the vertical axis.

Introduction

Vibratory conveyors are highly used for discharging, conveying, feeding, dosing and distributing bulk materials in many branches of industry, for example in the chemical and synthetic materials industries, food processing (Fig. 1(a)), sand, gravel, and stone quarries, for small-parts assembly mechanics (Fig. 1(b)), the paper-making industry, sugar or oil refineries, and foundries [1-3]. In addition to transport, vibration can be utilized to screen, separate, compact or loosen product. Open troughs are used for conveying bulk materials, closed tubes for dust-sealed goods, and work piece-specific rails for conveying oriented parts. Some of the main advantages of vibratory conveyors are their simple construction and their suitability to handle hot and abrasive materials. In addition, they are readily used in the food industry, since they can easily be kept complying to hygienic standards by using stainless steel troughs. Some disadvantages of vibratory conveyors are their noisy operation, the induced vibrations on their.

A quick return mechanism such as the one seen below is used where there is a need to convert rotary motion into reciprocating motion. As the disc rotates the black slide moves forwards and backwards. Many

machines have this type of mechanism and in the school workshop the best example is the shaping machine.

Conveying principles

Three different principles of conveying have to be distinguished

Sliding: Here the deck is moved by a crankshaft mechanism only horizontally

with asymmetric forward and backward motions. The material remains always in contact with the trough surface and is transported forward relative to the deck by a stick-slip drag.

Throwing: If the vertical component of the acceleration exceeds gravity, the material loses contact during part of the conveying cycle and is repeatedly forced to perform ballistic flights. Complicated sequences of a rest phase, a positive (or negative) sliding phase, and a flight phase have to be considered. The net transport in the forward (or even backward) direction depends sensitively on the coefficient of friction between the particles and the trough and on the coefficient of restitution for the collision with the deck.

² **Ratcheting:** Motivated by advances in the investigations of fluctuation-driven ratchets a new transport mechanism has been proposed recently a horizontal transport of granular particles can be achieved in a purely vertically.

Types of conveying system

- Gravity conveyor
- Gravity skate wheel conveyor
- Belt conveyor
- Wire mesh conveyors
- Plastic belt conveyors
- Bucket conveyors
- Flexible conveyors
- Vertical conveyors
- Spiral conveyors
- Vibrating conveyors

Types of conveyor system

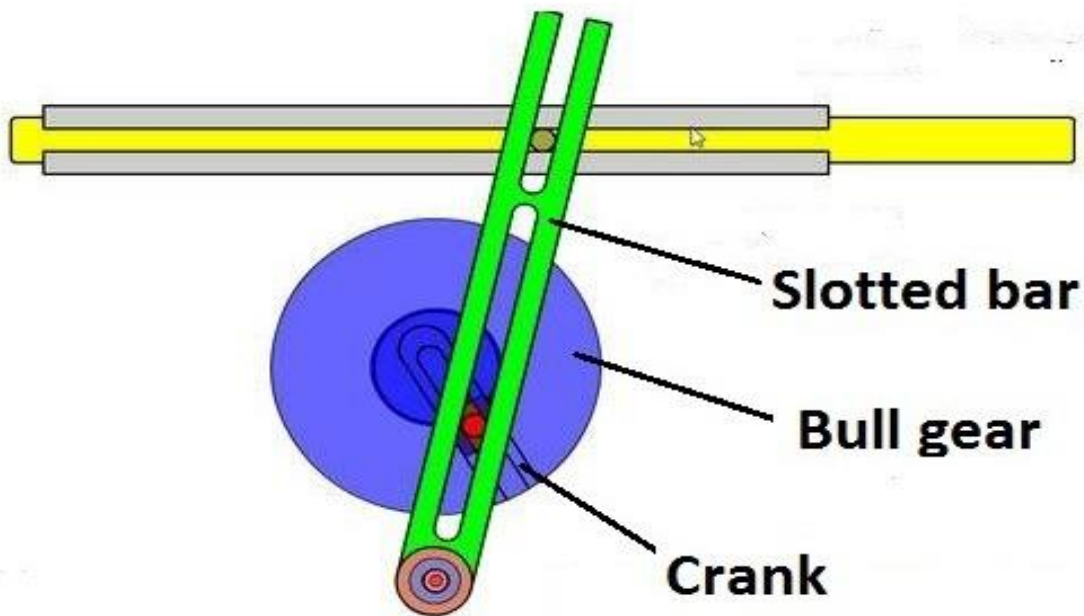
- Pneumatic conveyors
- track vehicle systems
- Belt driven live roller conveyors
- Line shaft roller conveyor
- Chain conveyor
- Screw conveyor or auger conveyor
- Chain driven live roller conveyor
- Overhead I-beam conveyors
- Dust proof conveyors
- Pharmaceutical conveyors
- Automotive conveyors
- Overland conveyor
- Drag Conveyor

Granular transport

Since the transport phenomena on vibratory conveyors involve the nonlinear interaction of many-particle systems with complex behavior, the investigation of their dynamical properties has become a challenging subject to physicists, too. In the past, most studies dealing with vibrated granular media were based on purely vertical or purely horizontal vibration. Only recently a few experimental explorations of the dynamics of granular beds subject to *simultaneous* horizontal and vertical vibration have been reported [3,8{14]. The observed phenomena include the spontaneous formation of a static heap, convective flow, reversal of transport, and self-organized spatiotemporal patterns like granular surface waves. The most important questions currently under investigation are:

1. How does the granular transport velocity depend on (i) *external* parameters of the drive like amplitude and frequency of the oscillation, the vibration mode, or the inclination of the trough, and (ii) *internal* bulk parameters like coefficient of restitution, friction coefficients, and the filling height?

2. Is it possible to optimize the transport efficiency by suitable modifications of the surface of the trough implying ratchet like profiles? What kind of self-organized structures can be expected? Are there clearly characterized instabilities? Which physical mechanism underlie these structures? How is the granular transport effected? Are there segregation effects in bidisperse or polydisperse systems? What are the analogies to vertical vibration? Can these results eventually lead to optimized industrial devices like conveyor systems, metering devices, sieves, mixers, dryers, or coolers?



Crank and slotted lever mechanism

Figure: A Quick Return Mechanism

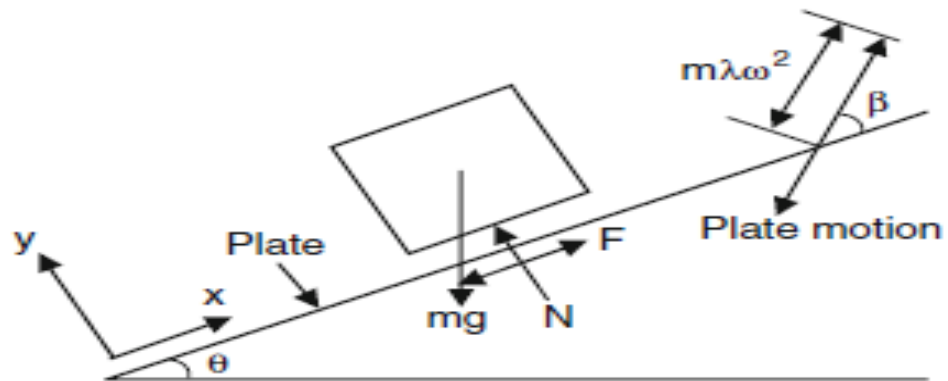
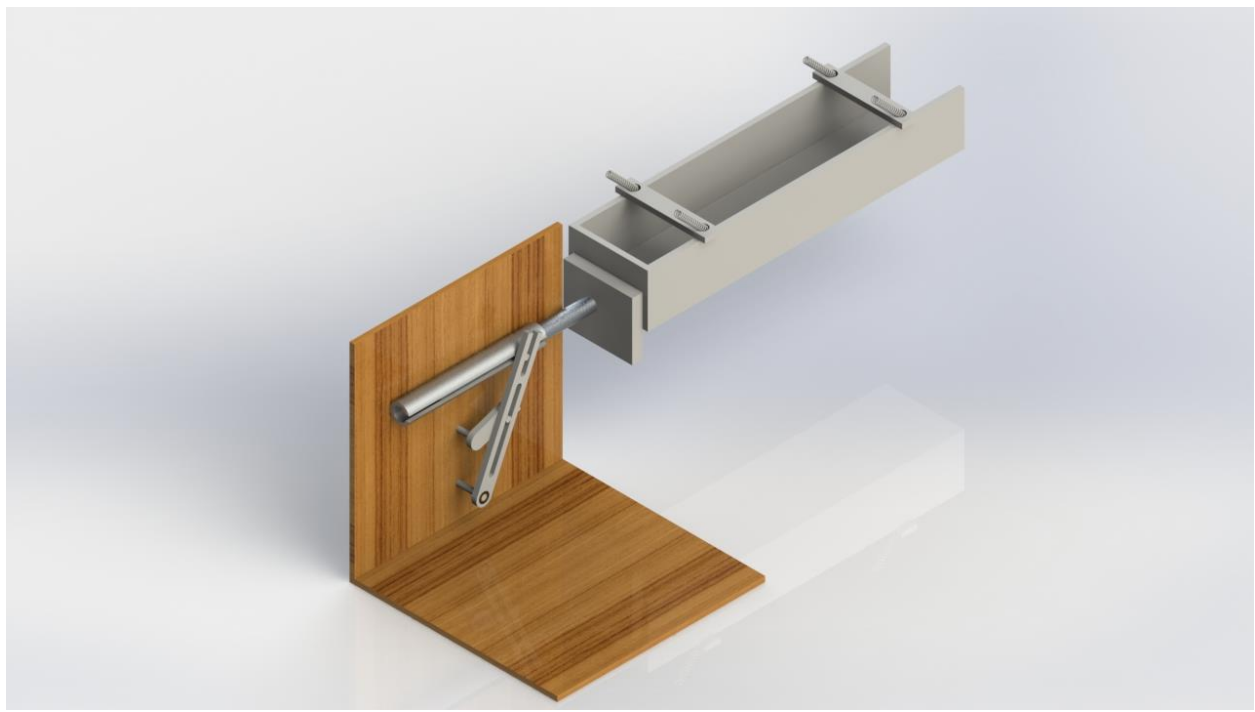


Fig. 4 The basic model and plate motion

Experimental Set-up



- The theoretical design shows the use of spring in quick return. But due to some constructional limitation along with time deficiency we had to use an MS shaft. The shaft connects the reciprocating bar with the tray.

- As the bar works in quick-return mechanism due to excessive inertia in the time of back stroke granular material (sand in this experiment) have greater forward moving tendency drives the granular material.

Materials Used:

- Wood frame
- Mild steel (Whitworth Mechanism)
- - GP sheet (4 mm) (Tray)

Design

- All mechanisms are formed upon the combination of two gears, where one drives the force of the other.^[3] The disc influences the force of the arm, which makes up the frame of reference of the quick return mechanism. The frame continues to an attached rod, which is connected to the circular disc. Powered by a motor, the disc rotates and the arm follows in the same direction (linear and left-to-right, typically) but at a different speed. When the disc nears a full revolution, the arm reaches its furthest position and returns to its initial position at a quicker rate, hence its name. Throughout the cut, the arm has a constant velocity. Upon returning to its initial position after reaching its maximum horizontal displacement, the arm reaches its highest velocity.
- The quick return mechanism was modeled after the crank and slider (arm), and this is present in its appearance and function; however, the crank is usually hand powered and the arm has the same rate throughout an entire revolution, whereas the arm of a quick return mechanism returns at a faster rate. The "quick return" allows for the arm to function with less energy during the cut than the initial cycle of the disc.

Specifications[\[edit\]](#)

- When using a machine that involves this mechanism, it is very important to not force the machine into reaching its maximum [stress](#) capacity; otherwise, the machine will break. The durability of the machine is related to the size of the arm and the velocity of the disc, where the arm might not be flexible enough to handle a certain speed. Creating a graphical layout for a quick return mechanism involves all inversions and motions, which is useful in determining the dimensions for a functioning mechanism.^[4] A layout would specify the dimensions of the mechanism by highlighting each part and its interaction among the system. These interactions would include [torque](#), force, velocity, and [acceleration](#). By relating these concepts to their respective analyses (kinematics and dynamics), one can comprehend the effect each part has on another.

Mechanics[\[edit\]](#)

- In order to derive the force vectors of these mechanisms, one must approach a mechanical design consisting of both kinematic and dynamic analyses.

Kinematic Analysis[\[edit\]](#)

Breaking the mechanism up into separate vectors and components allows us to create a kinematic analysis that can solve for the maximum velocity, acceleration, and force the mechanism is capable of in three-dimensional space.^[5] Most of the equations involved in the quick return mechanism setup originate from [Hamilton's principle](#).^[6]

- The position of the arm can be found at different times using the substitution of [Euler's formula](#):^[7]
-
- into the different components that have been pre-determined, according to the setup.
- This substitution can solve for various radii and components of the displacement of the arm at different values. [Trigonometry](#) is

needed for the complete understanding of the kinematic analyses of the mechanism, where the entire design can be transcribed onto a plane layout, highlighting all of the vector components.

- An important concept for the analysis of the velocity of the disc relative to the arm is the [angular velocity](#) of the disc:

[\[6\]](#)

- If one desires to calculate the velocity, one must derive the angles of interaction at a single moment of time, making this equation useful.

-

- **Dynamic Analysis**[\[edit\]](#)

- In addition to the kinematic analysis of a quick return mechanism, there is a dynamic analysis present. At certain lengths and attachments, the arm of the mechanism can be evaluated and then adjusted to certain preferences. For example, the differences in the forces acting upon the system at an instant can be represented by [D'Alembert's principle](#). Depending on the structural design of the quick return mechanism, the [law of cosines](#) can be used to determine the angles and displacements of the arm. The ratio between the working [stroke \(engine\)](#) and the return stroke can be simplified through the manipulation of these concepts.[\[9\]](#)
- Despite similarities between quick return mechanisms, there are many different possibilities for the outline of all forces, speeds, lengths, motions, functions, and vectors in a mechanism.

Friction Models

The Coulomb friction model describes the frictional force between two bodies that are in contact with each other. It uses only a single parameter to do so, namely the coefficient of friction. Two different cases may occur depending on the relative motion of the two bodies: Static friction and sliding friction.

Static Friction

Static friction applies when the two bodies in contact are at rest, i. e. when their relative velocity v_r is zero. It is assumed that a force F applies to the body (Figure 3.4). Its component perpendicular to the contact surface is called F_P and its tangential component F_T . The distribution of the surface pressure between the body and the supporting base is in most cases unknown, and is substituted by the normal force F_N [BG97]. The same is true for the distributed frictional force. It is substituted by the frictional force F_R .

Depending on the surface properties and the spatial inhomogeneity of the coefficient of friction, the lines of action of F_N and F_R do not necessarily need to cross each other. Figure 3.5 shows the effect of a very inhomogeneous distribution of the coefficient of friction. The three orthogonal views show a cubic object lying on a flat surface. It is assumed that the coefficient of friction is zero on one half of the contact surface and non-zero on the other half. This causes the point of attack of the resultant F_R of the distributed frictional force to be off-centered. As a result, F_T and F_R cause a moment about the vertical axis that can make the object

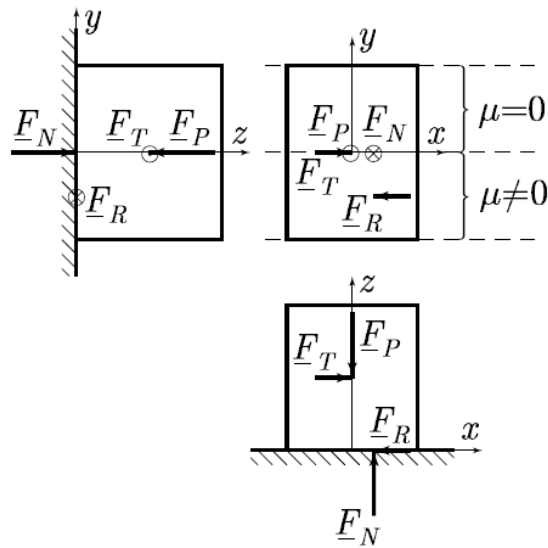


Figure 3.5: Local changes of the coefficient of friction may cause a turning moment to act on an object. The figure shows three perpendicular views; vectors pointing towards the reader are denoted by \odot , those away from the reader by \otimes .

In reality, the differences in the contact parameters are not as large as in this (hypothetical) example but the effect is the same. The parameters of the inhomogeneous contact cannot be directly determined experimentally. At the best, they could be estimated from an eventual rotation of the object. The result of such a measurement would be restricted to one specific object/surface pair and a certain surface region only. Changing conditions caused by wear of the surfaces, small depositions of dirt or divergences in the humidity would make the general applicability of the collected data questionable. The spatial inhomogeneity of the contact parameters is therefore not considered in this model. They are assumed to be constant hereafter. The equilibrium condition normal to the contact surface yields

The coefficient of static friction depends upon many factors, the most important ones being the type of materials in contact, the composition of their surfaces and presence of a lubricant μ_m .

The latter case can apply only instantaneously as it results in a net

horizontal force acting upon the object. Due to the net force, the object accelerates, causing its velocity to become non-zero at the very next instant.

Sliding Friction

In the situation shown in Figure 3.6, the supporting surface has a nonzero velocity v_r relative to the object. The force F that applies to the body is again divided into its two components F_P and F_N . As before, the distribution of the surface pressure between the body and the supporting base is unknown and substituted by F_N and F_R . Again, the equilibrium condition yields.

Contact Models

It is assumed that the bottom face of the object to be transported is a flat surface. Two different contact models need to be considered, depending

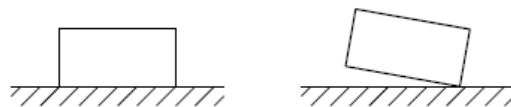


Figure 3.7: *Planar contact and point contact.*

upon the relative orientation of the object and the manipulator surface: Planar contact and point contact. The contact models are independent of the friction models. For each contact model, either static friction or sliding friction may apply.

Planar Contact

Planar contact is used if the object lies flat on the manipulator surface. The distributed contact force that applies to the object is substituted by the two forces F_N and F_R as described in Sections 3.2.1 and 3.2.2. Due to the fact that the distribution of the surface pressure is

not known, the point of application of the normal force F_N is not known, either. The unknown variable d (cf. Figure 3.4) is thus introduced to describe the horizontal distance between the object's center of gravity and the point of application of the normal force.

Point Contact

Point contact is applicable if the object is inclined against the horizontal plane (Figure 3.7). It is assumed that the inclined object has a shape that results in only a single point of contact with the manipulator surface, as is the case with a cylindrical object, for example. As a consequence, the point of application of the contact force is known exactly. Therefore, there is no need for a distributed force or a distance d in this case.

Theoretical description

Such a theoretical approach is based on the following initial assumptions [3,15,16]: The granular material behaves like a solid body and can be represented by a point mass.

1. When the layer of granular material hits the trough after a π phase a fully non-elastic collision is assumed.
2. Rotations of the particle and interactions with the side walls of the trough are neglected.
3. The kinetic and static coefficients of friction are set equal or the distinction between them is neglected.

² The air resistance during the π phase is negligible. According to these assumptions, Slood and Krut [3] obtained fairly good agreement between theory and experiment for slide conveyors but observed large deviations for linear throw conveyors with vibration angle. They described the dynamics of a vibratory feeder by a set of coupled, nonlinear and strongly dissipative mappings and identified the transport behavior to be determined by periodic and chaotic solutions. First simulations for conveyors with variable vibration mode (linear, circular, and elliptic) by

forces and collisions with complete dissipation of the vertical velocity component in order to understand the theoretical basics of the transport process led to rather good agreement with the experimental results shown

Onset of particle motion

Despite the complex interactions between the particles and the vibrating trough during the transport process, which up to now can only be handled via numerical simulations, it is interesting that the *onset* of motion for a single block subject to static friction can be derived analytically.

A *linear* harmonic motion of the conveyor with amplitude A and vibration angle θ (see inset of Fig. 9(a)) can be expressed as $x(t) = A \cos(\theta) \cos(2^{1/4} \omega t)$ for its horizontal and $y(t) = A \sin(\theta) \cos(2^{1/4} \omega t)$ for the vertical component, respectively. Due to the periodic acceleration a particle with mass m lying on the trough experiences a horizontal force $F_h(t) = m \ddot{x}(t)$ and a modulated effective weight $N(t) = m(g + \ddot{y}(t))$. The mass is hindered from sliding if the resulting frictional force $F(t) = \mu_s N(t)$ is larger than $|F_h(t)|$, where μ_s is the static coefficient of friction. At the onset of particle motion both forces are equal, which leads to the balance equation

$$|m \ddot{x}(t)| = \mu_s m (g + \ddot{y}(t)) \quad (2)$$

Materials to be conveyed

Granular transport

The most important questions currently under investigation are:

* How does the granular transport velocity depend on (i) *external* parameters of the drive like amplitude and frequency of the oscillation, the vibration mode, or the inclination of the trough, and (ii) *internal* bulk parameters like coefficient of restitution, friction coefficients, and the falling height?

* Is it possible to optimize the transport affectivity by suitable modifications of the surface of the trough implying ratchet like profiles?

Observations:

Data Collected:

Table 2 Theoretical mean conveying velocity when track angle is 0°

S. no.	f (Hz)	ω (rad/s)	λ (mm)	Mean conveying velocity (mm/s)						
				$\mu=0.1$	$\mu=0.2$	$\mu=0.3$	$\mu=0.4$	$\mu=0.5$	$\mu=0.6$	$\mu=0.7$
1	30	188.57	0.644	43.593	54.491	62.967	67.811	72.655	77.498	82.342
2	35	220.00	0.473	37.365	46.707	53.972	58.124	62.276	66.427	70.579
3	40	251.43	0.362	32.695	40.868	47.226	50.858	54.491	58.124	61.757
4	45	282.86	0.286	29.062	36.327	41.978	45.207	48.437	51.666	54.895
5	50	314.29	0.232	26.156	32.695	37.78	40.687	43.593	46.499	49.405
6	55	345.71	0.192	23.778	29.722	34.346	36.988	39.63	42.272	44.914
7	60	377.14	0.161	21.796	27.246	31.484	33.906	36.327	38.749	41.171

From the analysis of forces, we may write

$$m\lambda\omega^2 \cos\beta > mg \sin\theta + F \quad (1)$$

$$F = \mu N = \mu(mg \cos\theta - m\lambda\omega^2 \sin\beta) \quad (2)$$

Combining Eqs. (1) and (2), for forward sliding,

$$\frac{\lambda\omega^2}{g} > \frac{(\mu \cos\theta + \sin\theta)}{(\cos\beta + \mu \sin\beta)} \quad (3)$$

and for backward sliding

$$\frac{\lambda\omega^2}{g} > \frac{(\mu \cos\theta - \sin\theta)}{(\cos\beta - \mu \sin\beta)} \quad (4)$$

Let us consider

$$\lambda_n = \lambda\omega^2 \sin\beta \quad (5)$$

$$g_n = g \cos\theta \quad (6)$$

The operating conditions can be expressed in terms of dimensionless normal plate acceleration as $\frac{\lambda_n}{g_n}$ which is given by

$$\frac{\lambda_n}{g_n} = \frac{\lambda\omega^2 \sin\beta}{g \cos\theta} \quad (7)$$

for forward sliding

$$\frac{\lambda_n}{g_n} > \frac{(\mu_f + \tan\theta)}{(\cot\beta + \mu_f)} \quad (8)$$

for backward sliding

$$\frac{\lambda_n}{g_n} > \frac{(\mu_f - \tan\theta)}{(\cot\beta - \mu_f)} \quad (9)$$

Now for sufficiently large amplitudes, the part will leave the plate and hop forward during each cycle. This will

happen when the reaction between the part and the plate becomes zero. Using Eq. (2),

$$N = 0 = mg \cos\theta - m\lambda\omega^2 \sin\beta \quad (10)$$

For the part to drop forward

$$\frac{\lambda\omega^2}{g} > \frac{\cos\theta}{\sin\beta} \text{ Or } \frac{\lambda_n}{g_n} > 1.0 \quad (11)$$

3.2 Motion of the trough

The typical hamonic motion of the trough used in a vibratory feeder is shown in Fig. 5. Here, a trough is constrained in such a way that it can move only in a direction perpendicular to the fixed guide springs. The line of motion of the trough is represented by S_T which makes an angle β with the horizontal. This angle, called the angle of oscillation or the drive angle, is generally about 20–30°.

The position of the trough oscillating at frequency f and amplitude λ at a given time t is represented

$$S_T = \lambda(1 - \cos 2\pi ft) \quad (12)$$

Table 3 Comparison of theoretical and actual conveying velocity of the feeder when track angle is 0°, coefficient of friction is 0.5, and vibration angle is 20°

S. no.	Frequency (Hz)	Theoretical mean conveying velocity (mm/s)	Actual conveying velocity (mm/s)		
			Square springs	Helical springs	Screw springs
1	30	72.655	63	68	60
2	35	62.276	58	59	57
3	40	54.491	49	50	47
4	45	48.437	41	45	44
5	50	43.593	39	41	42
6	55	39.630	31	32	34
7	60	36.327	26	28	30

The acceleration of the trough in the direction of oscillation is

$$\ddot{S}_T = \frac{d^2 S_T}{dt^2} = \lambda(2\pi f)^2 \cos 2\pi ft \quad (13)$$

The horizontal and vertical displacements of the trough at time t can be written

$$x_T = \lambda(1 - \cos 2\pi ft) \cos \beta \quad (14)$$

$$y_T = \lambda(1 - \cos 2\pi ft) \sin \beta \quad (15)$$

Also the horizontal and vertical components of the acceleration of the trough can be determined by

$$\ddot{x}_T = \lambda(2\pi f)^2 \cos 2\pi ft \cos \beta \quad (16)$$

$$\ddot{y}_T = \lambda(2\pi f)^2 \cos 2\pi ft \sin \beta \quad (17)$$

The bulk material which is being conveyed will be lifted off the surface of the trough when the acceleration of the trough in the downward vertical direction becomes equal to the gravitational acceleration g

$$\ddot{y}_T = -g \quad (18)$$

The time at which this occurs is then given by

$$t_1 = \frac{1}{2\pi f} \cos^{-1} \left[\frac{-g}{\lambda(2\pi f)^2 \sin \beta} \right] \quad (19)$$

While in flight, the particles will tend to follow a parabolic trajectory to the next impact point, after which they will be carried forward and upward for a short interval before being thrown again when the trough decelerates. For the most efficient operation of the conveyor there should be no backward movement of the components at any part of the cycle and therefore the impact point should coincide with the start of the flight phase.

An important parameter in the modeling of vibratory conveyors is therefore the ratio of the vertical acceleration

of the trough and the gravitational acceleration (g). This ratio determines the point at which the flight phase begins. The maximum value of this parameter will be determined at the design stage by selecting the chosen value of frequency, amplitude, and the angle of oscillation. This parameter called the 'dynamic material coefficient' Γ and is determined by

$$\Gamma = \frac{\ddot{y}_{T \max}}{g} = \frac{\lambda(2\pi f)^2 \sin \beta}{g} \quad (20)$$

At the start of the flight phase $y_T / g = -1$, and it follows that, if the value of Γ is less than unity, the bulk solid will not leave the surface of the trough and forward movement will be negligible.

Another essential consideration when selecting the operating condition of a vibratory conveyor is the relationship between the frequency and the amplitude of oscillation. In general, the higher the frequency, the smaller will be the amplitude. It is convenient to express the relationship in terms of the ratio of the maximum trough acceleration

Table 5 Comparison of theoretical and actual conveying velocity of the feeder when track angle is 4°, friction coefficient is 0.5, and vibration angle is 20°

S. no.	Frequency (Hz)	Theoretical mean conveying velocity (mm/s)	Conveying velocity (mm/s)		
			Square springs	Helical springs	Screw springs
1	30	90.818	70	70	65
2	35	77.844	67	67	63
3	40	68.114	62	62	62
4	45	60.546	56	56	57
5	50	54.491	50	50	52
6	55	49.537	42	42	49
7	60	45.409	40	40	45

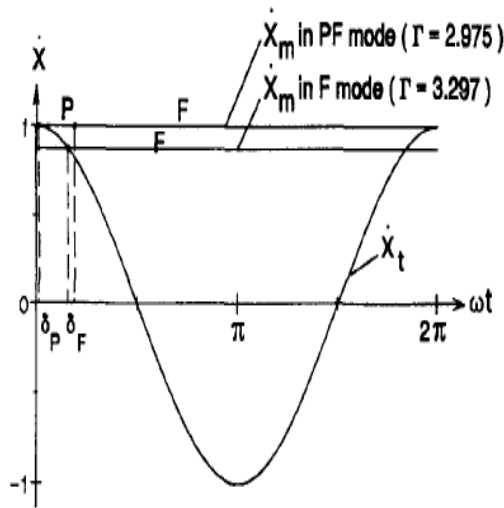


Fig. 6. Tangential velocities of trough and point mass as a function of time (large throw numbers).

Fig. 6. The dependence on μ and $\tan\beta$ seems to be very small, especially for horizontal transport [8]. Since the maximum velocity efficiency is obtained for $\Gamma=2.975$, it is not useful to design a vibratory conveyor with a throw number larger than 3.0.

3.5. Limiting case of small vibration angles for slide phases

In this section the case of a small vibration angle is studied in order to derive a relation that describes the influence of inclination on the velocity efficiency for small vibration angles. Furthermore, a method is described to measure the friction coefficient between granular material and trough.

Equations for the start and end of a *PN* mode, which implies $\delta_N = \epsilon_p$ and $\epsilon_N = \delta_p + 2\pi$, are obtained from Eq. (11):

$$\sin(\delta_p + 1/2C) = \frac{(C - 2\pi) \sin \delta_3}{2 \sin(1/2C)}$$

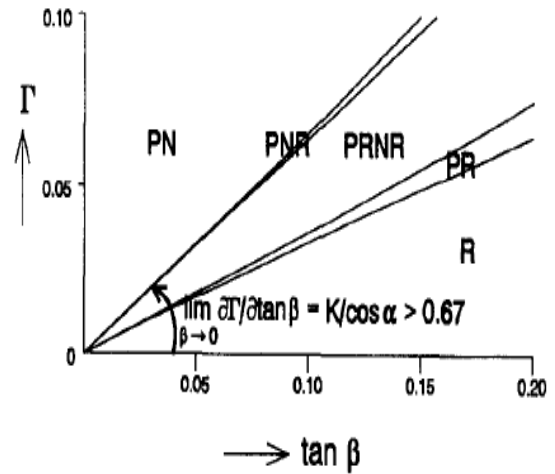


Fig. 7. Mode diagram for small vibration angles ($\alpha=0$, $\mu=0.35$).

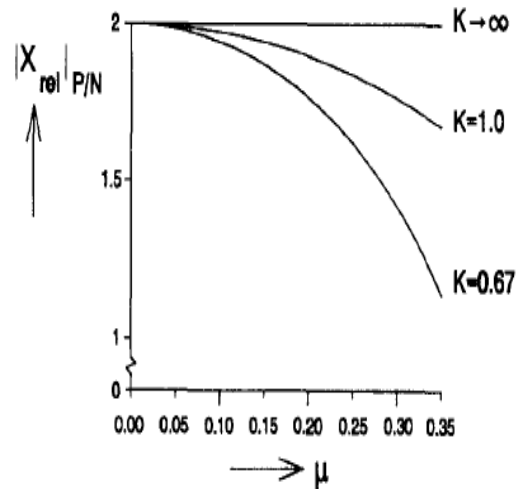


Fig. 8. Maximum relative displacement for a *PN* mode, as a function of friction coefficient μ and machine number K .

for infinite values of the machine number, it follows after some algebra from Eqs. (4), (8), (10) and (20) that the limiting value of the efficiency for each inclination or declination angle is given by:

$$\eta_{\beta \rightarrow 0} = -\cos\left(\frac{C}{2}\right) = -\sin\left(\frac{\pi \tan \alpha}{2\mu}\right) \quad (21)$$

Symbol	Description
$\underline{\underline{A}}$	Feedback matrix of a dynamic system (state space representation)
A, A^*	Point on the edge of a calibration tetragon
$\underline{\underline{A}}_B$	Feedback matrix of the observer
$\underline{\underline{B}}$	Input matrix of a dynamic system (state space representation)
B, B^*	Point on the edge of a calibration tetragon
$\underline{\underline{B}}_B$	Input matrix of the observer
c	Index of the current column number
\bar{c}	Column coordinate of the object's center of gravity
c_0, c_1	Column indices of an object's boundary pixels
c_1, c_2	Abbreviations for trigonometric expressions containing the cardanic angles
c_x, c_y	Integration constants
$c_\theta, c_\psi, c_\phi, c_\nu$	Abbreviations for the cosine of these angles
$\underline{\underline{C}}$	Output matrix of a dynamic system (state space representation)
C, C^*	Point on the edge of a calibration tetragon
$\underline{\underline{C}}_B$	Output matrix of the observer
d	Distance between two objects on the manipulator surface
\underline{d}	Object property vector
\bar{d}	Offset of the normal force's point of application
d_f	Focal length of the camera's lens
\underline{d}_n	Normalized object property vector
d_m	Distance between the camera and the manipulator surface
$\underline{\underline{D}}$	Feed-through matrix of a dynamic system (state space representation)
D, D^*	Point on the edge of a calibration tetragon
$\underline{\underline{D}}_B$	Feed-through matrix of the observer
$e_{\bar{c}}, e_{\bar{l}}$	Random variables describing the error of the actual and the calculated center of gravity of an object
$f(c, l)$	Mathematical representation of a camera image
\underline{F}	Contact force applying to the object
$\underline{\underline{F}}$	Feedback matrix of a discrete-time dynamic system

Graph Plotted:

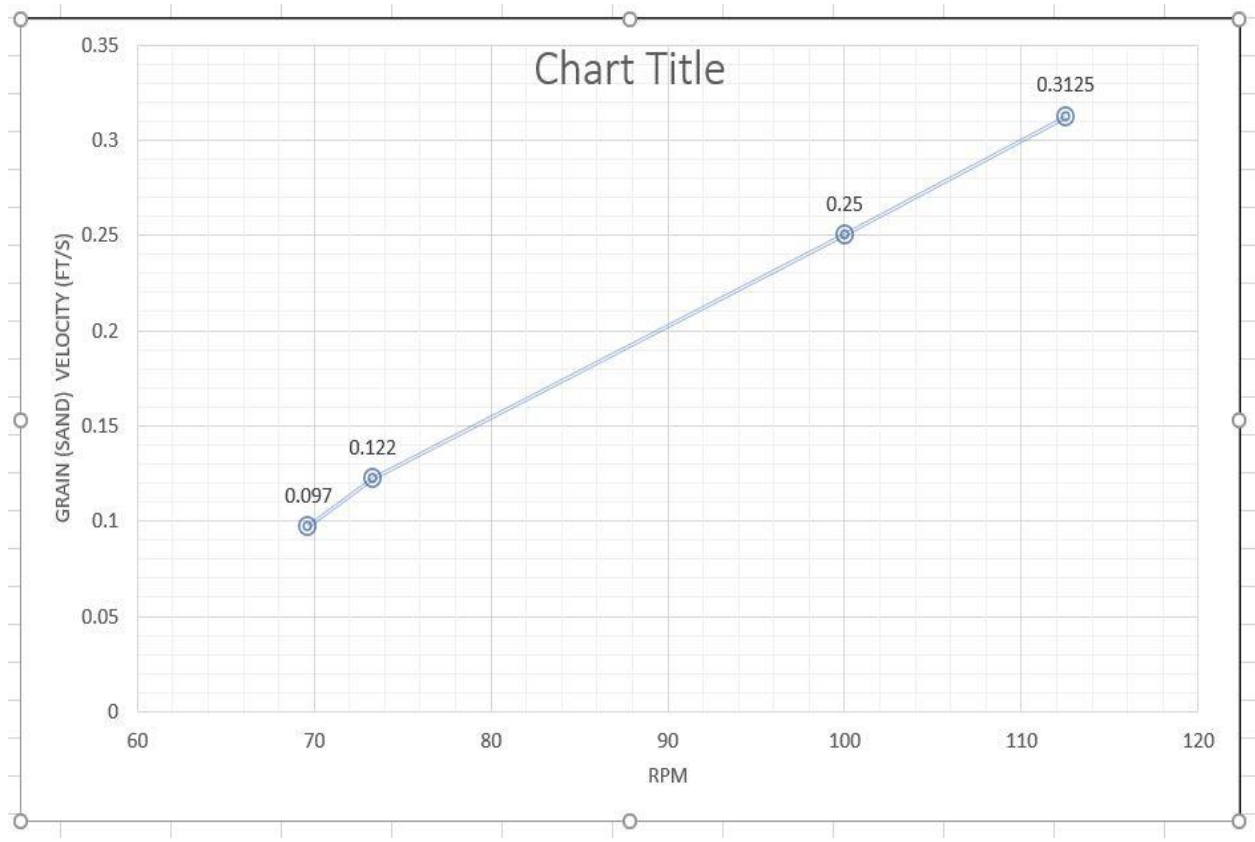


Figure: Velocity Of grain Versus RPM

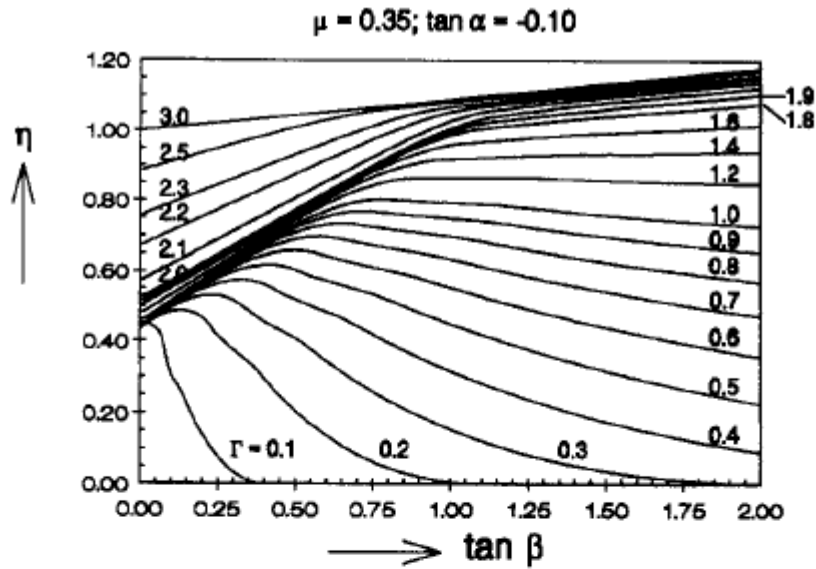


Fig. 3. Velocity efficiency for declined transport as a function of vibration angle β and throw number Γ .

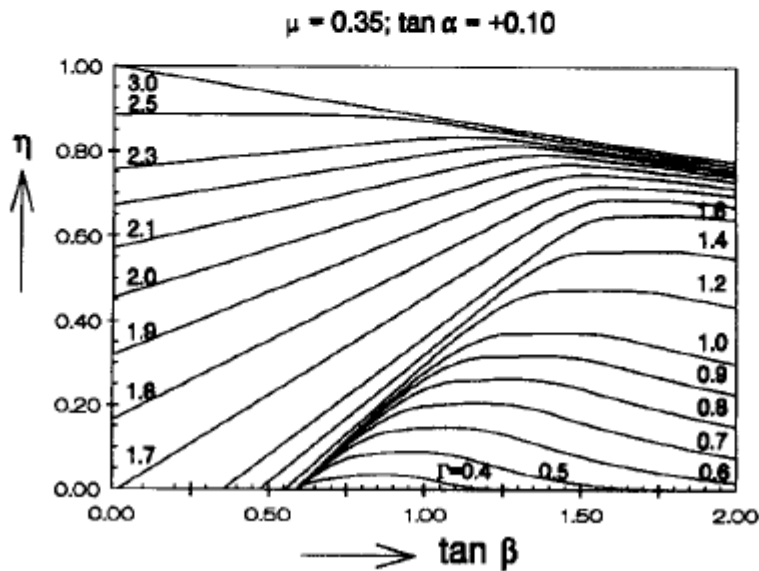


Fig. 4. Velocity efficiency for inclined transport as a function of vibration angle β and throw number Γ .

Experiments were conducted for the range of frequency of vibration (30–60Hz), feed track angles (0° and 4°), and the actual conveying velocity of the feeder was measured for square spring, helical spring, and screws. Theoretical values of conveying velocity of feeder were calculated using the proposed model and compared with measured values. The

theoretical mean conveying velocity of the feeder for different coefficients of friction was given in Table 2 for track angle 0° . The theoretical and actual conveying velocities at 0.5 coefficient of friction, 20° vibration angle and 0° track angle were compared in Table 3. Similarly, Table 4 shows the theoretical mean conveying velocity at different coefficients of friction at track angle 4° . The theoretical values are compared with actual conveying velocity in Table 5.

4.1 Effect of frequency of vibration on conveying velocity

Theoretical and measured values of conveying velocity of the feeder for the track angle 0° and 4° are plotted in Fig. 7a and b. It is observed that the conveying velocity estimated by the proposed model decreases with increase in frequency of vibration. The actual values of the conveying velocity also follow the same trend when the frequency of vibration is increased from 30 to 60Hz. From the theoretical analysis, it is found that, for constant track acceleration, the mean conveying velocity is inversely proportional to the vibration frequency. Hence, for attaining high conveying velocities and high feed rates, it is desirable to use as low frequency as possible. Hence, in the present feeder, it is desirable to use frequency of vibration above 35Hz for achieving high yield.

Effect of amplitude of vibration on conveying velocity

The effect of amplitude of vibration on mean conveying velocity is shown in Fig. 8a and b. Proposed model and theoretical analysis show that, for small amplitudes of vibration, the conveying velocity will be low as the part will remain stationary on the track and its inertia force will be too small to overcome the frictional force. At sufficiently larger amplitudes of vibration, the part leaves the track, hence the conveying velocity will be high. In Section 4.1, it has been noted that as the frequency decreases the conveying velocity increases. To maintain track acceleration, the amplitude must

be increased. However, when the amplitude is increased beyond 0.6 mm, there is no significant increase in the conveying velocity as the dimensionless normal acceleration reaches its limiting value for the forward sliding of the part to occur on the track. This condition has been derived in the theoretical model as given by Eq. (11).

Effect of coefficient of friction on conveying velocity

From Figs. 7a, b and 8a, b, it is observed that the mean conveying velocity of the feeder increases with increase in coefficient of friction. It can also be seen from Fig. 7a that a near linear relationship exists between the frequency of vibration and the mean conveying velocity for coefficient of friction from 0.1 to 0.7. The coefficient of friction depends on the nature of the conveying bed used in the feed track on which the components will be sliding. In the present experiment, a rubber lining is used to increase the coefficient of friction to approximately 0.7. This resulted in increase in mean conveying velocity of the track and reduction in the noise level of the system.

Effect of track angle on conveying velocity

It is also observed from Fig. 7a, b and Tables 2 and 4 that, when the track angle is increased from 0° to 4° , there is a considerable increase in the conveying velocity of feeder for the given frequency of vibration. Similar increase in conveying velocity is also seen in Fig. 8a and b. Increase in feed track angle with respect to horizontal increases the forward sliding velocity of components and hence the components tend to move at faster rate.

Theoretical conveying velocity predicted by the proposed model is plotted against actual conveying velocity for

Design Modification Scope

- As the pin is fixed in a higher position , the stroke length is larger. It is possible to make the arrangement in such a way where pin position can be changed and shorter stroke length can be attained. This will cause higher Grain velocity in the same RPM.



- The tray can be set up on a rail which will cause less friction and thus smoother grain transfer
- **Friction Reduction Coatings.** Master Bond's **friction reduction coatings** can be applied to a wide variety of substrates to **reduce** wear and abrasion. Specialty low coefficient of **friction** epoxy **coatings** can be applied on metal, glass, plastic substrates. They provide durable, slippery surfaces and **reduce** wear/abrasion and smoother and faster Transfer of granular materials.



Advantages:

- Simple construction
- Suitable for handling hot and abrasive material
- they are readily used in the food industry, since they can easily be kept complying to hygienic standards by using stainless steel troughs

Disadvantages:

- Noisy operation
- induced vibration on their surrounding
- limited transport distance
- Furthermore, the granular material may be damaged when it is subjected to extreme accelerations normal to the trough.

Concluding remarks

The vibratory conveyor system presented here opens up the possibility to investigate the transport properties of granular materials in a systematic way. Our results show that under certain conditions not even the direction of the granular flow can be predicted a priori. The delicate interactions of the particles with the

support as well as among themselves have to be taken into account.

For industrial applications, the observed reversal effect is relevant as the direction of a granular flow is selected through the frequency of the excitation alone. One can employ such two-way conveyors for example in larger cascading transport systems as control elements to convey the material to different processes as needed.

These experiments indicate that the major concepts describing the complex behavior of a vibrated granular system, namely phase transitions, pattern formation, and transport are closely related and yield a rewarding yield for future research.

Various experiments were conducted for investigating the influence of various parameters such as track angle, coefficient of friction, frequency, and amplitude of vibration on the conveying velocity. The influence of these factors predicted by the theoretical model agreed well with the experimental values. The correlation coefficient between actual velocity and theoretical velocity is very high.

From the experiments, it is observed that the coefficient of friction has a significant influence on conveying velocity. In order to achieve higher conveying velocity, a rubber lining is provided on the track. The mean conveying velocity at 35 Hz operating frequency is found to be suitable while conveying springs and screws. The proposed method can be used for predicting and optimizing the time

required for conveying the small parts.

1. Stroke length affects the grain velocity . Higher stroke length will cause smaller velocity in the same RPM

2. The thickness of the tray sheet metal should be considered wisely . Higher thickness will cause hindrance to the tray vibration whereas too low thickness can get easily damaged.

3. Optimum thickness should be chosen.

The graph shows that the grains don't have significant movement before a certain RPM. That threshold value was found 48 RPM.

References

1. G. Pajer, H. Kuhnt, F. Kuhnt: *FÄordertechnik { StetigfÄorderer*, 5th edn. (VEB Verlag Technik, Berlin 1988)
2. F.J.C. Rademacher, L. Ter Borg: *Eng. Res.* 60, 261 (1994)
3. E.M. Sloot, N.P. Kruyt: *Powder Technol.* 87, 203 (1996)
4. A.W. Gerstel, J.G.R. Scheublin: *Bulk Solids Handling* 14, 573 (1994)
5. I. Derényi, P. Tegzes, T. Vicsek: *Chaos* 8, 657 (1998)
6. Z. Farkas, P. Tegzes, A. Vukics, T. Vicsek: *Phys. Rev. E* 60, 7022 (1999)
7. F.J.C. Rademacher: *Bulk Solids Handling* 15, 41 (1995)
8. S.G.K. Tennakoon, R.P. Behringer: *Phys. Rev. Lett.* 81, 794 (1998)
9. R. Grochowski, S. Strugholtz, P. Walzel, C.A. KrÄulle: *Chemie Ingenieur Technik* 75, 1103 (2003)
10. M. Rouijaa, C. KrÄulle, I. Rehberg, R. Grochowski, P. Walzel: *Chemie Ingenieur Technik* 76, 62 (2004)
11. M. Rouijaa, C. KrÄulle, I. Rehberg, R. Grochowski, P. Walzel: *Chem. Eng. Tech.* 28, 41 (2005)
12. R. Grochowski, P. Walzel, M. Rouijaa, C. A. Kruelle, I. Rehberg: *Appl. Phys. Lett.*

84, 1019 (2004)

13. R. Grochowski, S. Strugholtz, H. El hor, S.J. Linz, P. Walzel: `Transport Properties of Granular Matter on Vibratory Conveyors'. In: *Proceedings of International*

Congress for Particle Technology (PARTEC 2004) at Nuremberg, March 16

14. C.A. Kruelle, M. Rouijaa, A. GÄotzendorfer, I. Rehberg, R.Grochowski, P. Walzel,

H. El hor, S.J. Linz: `Reversal of a Granular Flow on a Vibratory Conveyor'. In:

Powders and Grains 2005, ed. by R. Garca-Rojo, H.J. Herrmann, S. McNamara

(Balkema, Leiden 2005) pp. 1185-1189

15. H. El hor, S.J. Linz: *J. Stat. Mech.* L02005 (2005)

16. H. El hor, S.J. Linz, R. Grochowski, P. Walzel, C.A. Kruelle, M. Rouijaa, A. GÄotzendorfer, I. Rehberg: `Model for Transport of Granular Matter on Vibratory

Conveyors'. In: *Powders and Grains 2005*, ed. by R. Garca-Rojo, H.J. Herrmann,

S. McNamara (Balkema, Leiden 2005) pp. 1191-1195

17. M.-O. Hongler, P. Cartier, P. Flury: *Phys. Lett.* 135, 106 (1989)

18. F. Landwehr, R. Lange, P. Walzel: *Chemie Ingenieur Technik* 69, 1422 (1997)

19. F. Landwehr, P. Walzel: *Chemie Ingenieur Technik* 71, 1167 (1999)

20. F. Melo, P.B. Umbanhower, H.L. Swinney: *Phys. Rev. Lett.* 75, 3838 (1995)

21. C.A. Kruelle, S. Auma³tre, A.P.J. Breu, A. Goetzendorfer, T. Schnautz, R. Gro-

chowski, P. Walzel: `Phase Transitions and Segregation Phenomena in Vibrated

Granular Systems'. In: *Advances in Solid State Physics* 44, ed. by B. Kramer

(Springer, Berlin 2004) pp. 401-414

22. A. Götendorfer, C.A. Kruelle, I. Rehberg: 'Granular Surface Waves in a Vibratory

Conveyor'. In: *Powders and Grains 2005*, ed. by R. Garca-Rojo, H.J. Herrmann,

S. McNamara (Balkema, Leiden 2005) pp. 1181-1184

23. S. Douady, S. Fauve, C. Laroche: *Europhys. Lett.* 8, 621 (1989)

24. H.K. Pak, R.P. Behringer: *Phys. Rev. Lett.* 71, 1832 (1993)

25. F. Melo, P. Umbanhowar, H.L. Swinney: *Phys. Rev. Lett.* 72, 172 (1994)

26. T. Metcalf, J.B. Knight, H.M. Jaeger: *Physica A* 236, 202 (1997)

27. P.B. Umbanhowar, F. Melo, H.L. Swinney: *Physica A* 249, 1 (1998)

28. C. Bizon, M.D. Shattuck, J.B. Swift, W.D. McCormick, H.L. Swinney: *Phys. Rev.*

Lett. 80, 57 (1998)

29. E. van Doorn, R.P. Behringer: 'Wavy Instability in Shaken Sand'. In: *Powders and*

Grains 1997, ed. by R.P. Behringer, J. Jenkins (Balkema, Leiden 1997) pp. 397-400

30. A. Götendorfer, J. Kreft, C.A. Kruelle, I. Rehberg: *Phys. Rev. Lett.* 95, 135704

(2005)